

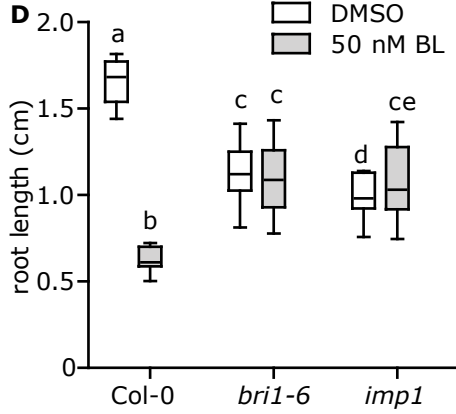
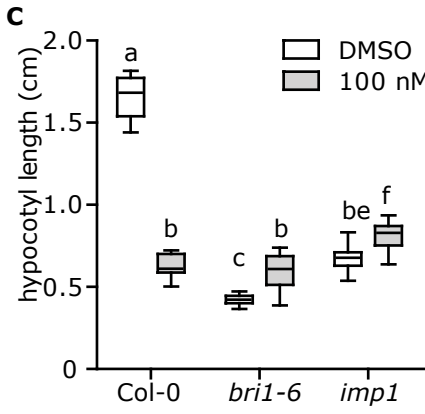
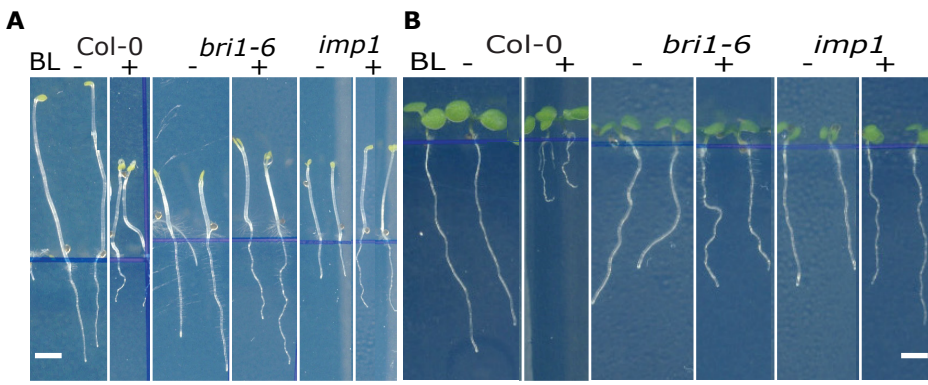
Current Biology, Volume 30

Supplemental Information

PIN-LIKES Coordinate Brassinosteroid Signaling

with Nuclear Auxin Input in *Arabidopsis thaliana*

Lin Sun, Elena Feraru, Mugurel I. Feraru, Sascha Waidmann, Wenfei Wang, Gisele Passaia, Zhi-Yong Wang, Krzysztof Wabnik, and Jürgen Kleine-Vehn



E Col-0 PILS5OE *imp1*; PILS5OE *bri1-6*; PILS5OE *bri1-6*

F Col-0 PILS5OE *imp1*; PILS5OE *bri1-6*; PILS5OE *bri1-6*

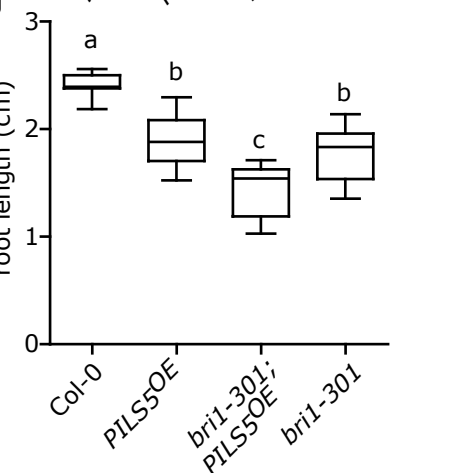
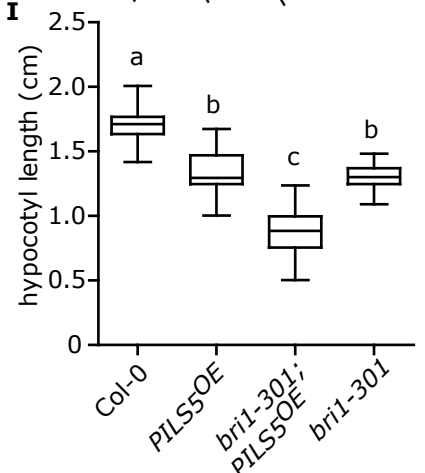
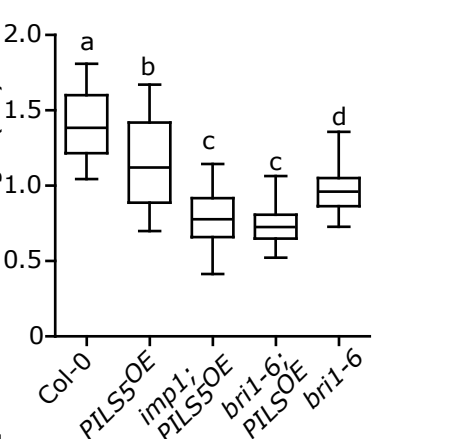
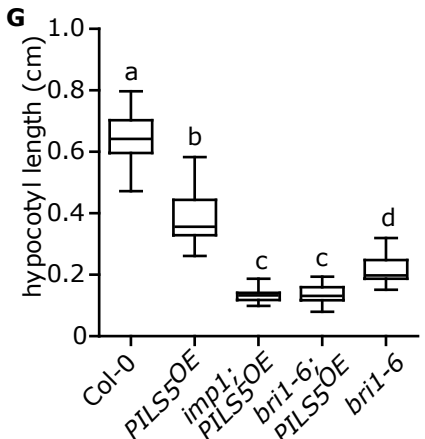
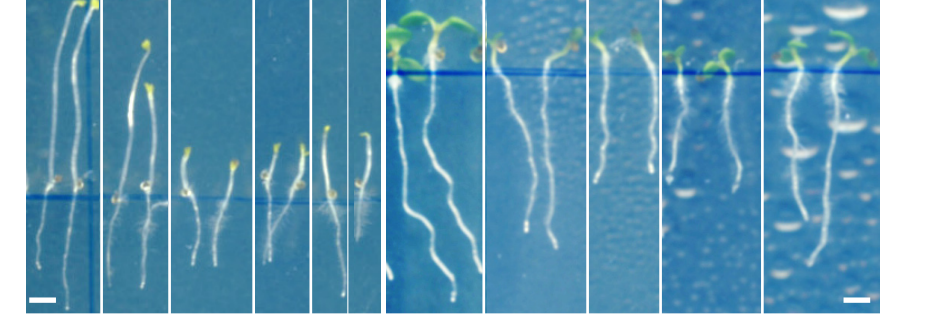


Figure S1. Impaired BR perception enhances *PILS5^{OE}* phenotypes. Related to Figure 2.

(A-D) Images and quantifications of 5-d-old dark-grown (A, C) and 6-d-old light-grown (B, D) seedlings of wild type (Col-0/WT), *bri1-6* and *imp1* germinated on plates with DMSO, 100 nM (A, C), or 50 nM BL (B, D). (n > 25). Scale bar, 3 mm. (E-H) Scanned images and quantifications of 5-d-old dark-grown (E, G) and 6-d-old light-grown (F, H) seedlings of WT, *PILS5^{OE}*, and *bri1* mutants. (n > 25). Scale bar, 3 mm. (I and J) Quantifications of 5-d-old dark-grown (I) and 6-d-old light-grown (J) seedlings of WT, *PILS5^{OE}*, and *bri1-301* mutants. Letters indicate values with statistically significant differences (P < 0.05, two-way ANOVA (C and D); P < 0.01, one-way ANOVA (G-J)).

Figure S2. Predicted BZR1 and BZR2 binding motifs in the promoters of *PILS2*, *PILS3*, and *PILS5*. Related to Figure 3.

Here, we have used JASPAR [54] which is an open-access database of curated, non-redundant transcription factor (TF) binding profiles stored as position frequency matrices (PFMs) and TF flexible models (TFFMs). JASPAR proposed certain probability of BZR binding for *pPILS2* ($p > 89\%$), *pPILS3* ($p > 80\%$), and *pPILS5* ($p > 90\%$) promoters. The *in silico* predicted G boxes, containing the core E-box motif (ACGT) and/or BZR motif (CGTG), are depicted in yellow (for BZR1) and blue (for BZR2) in *PILS2*, *PILS3*, and *PILS5* promoter sequences.

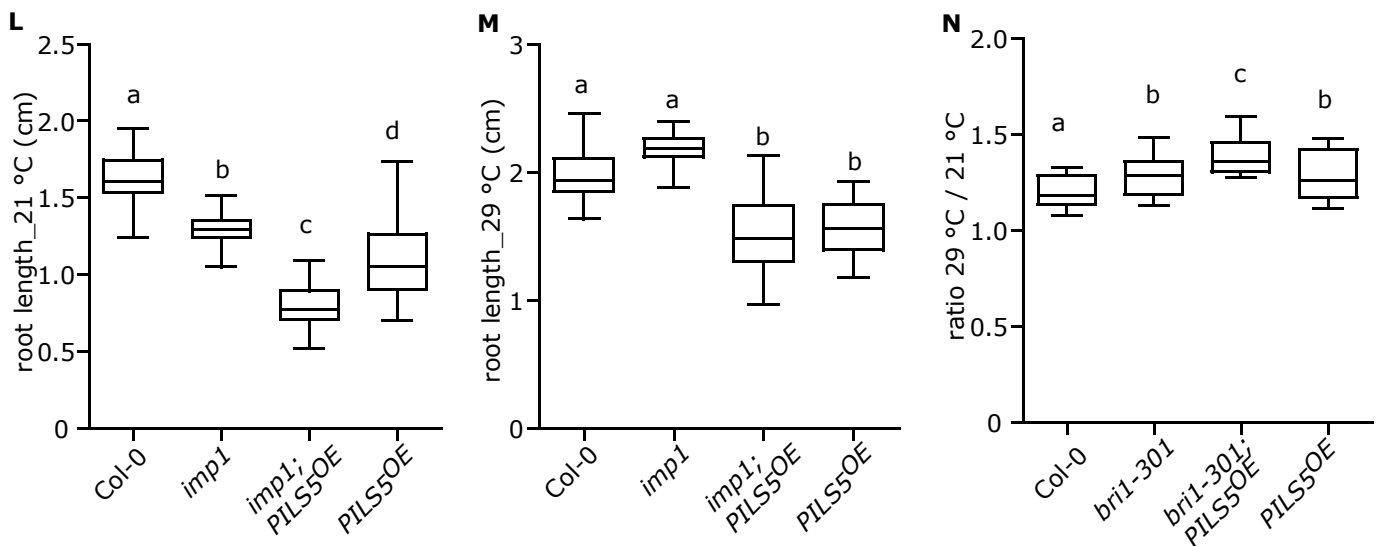
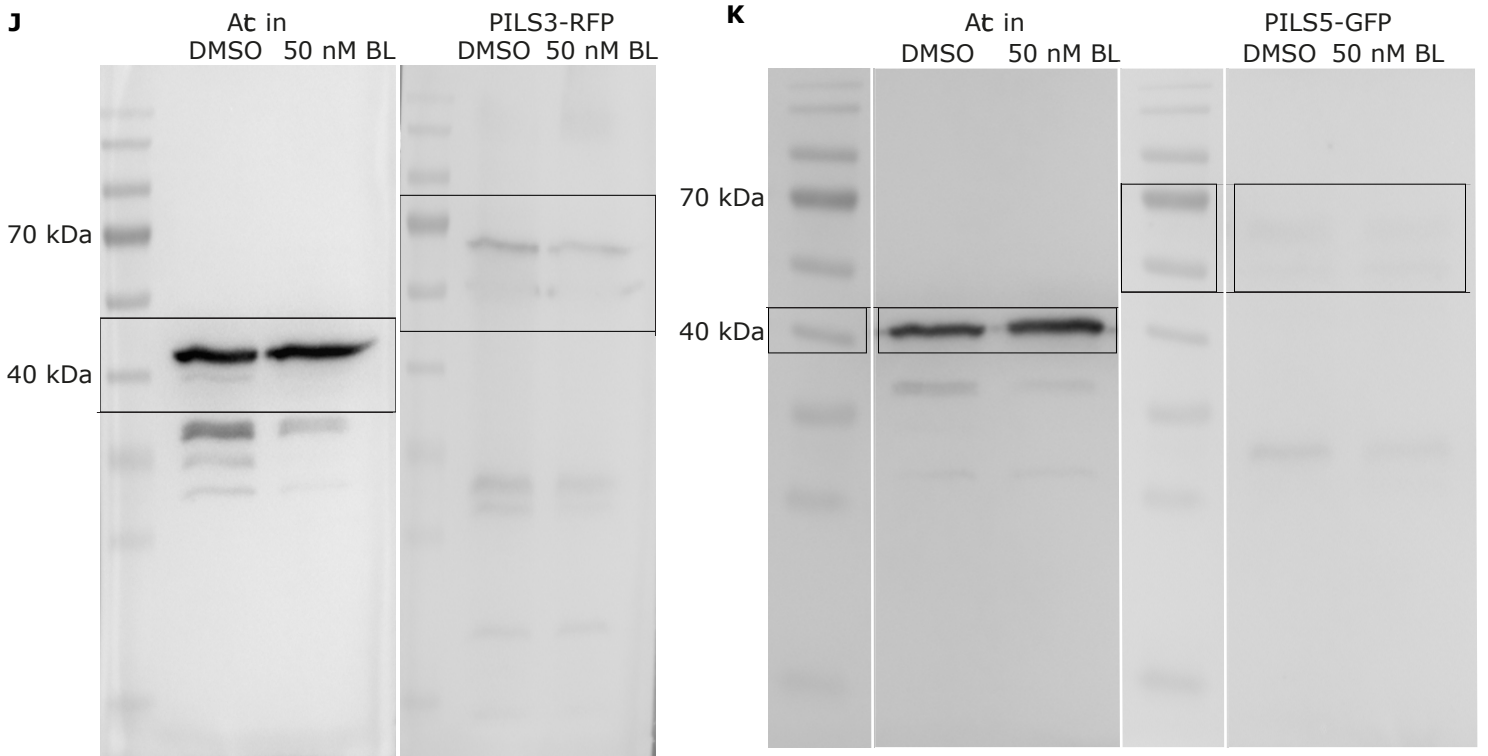
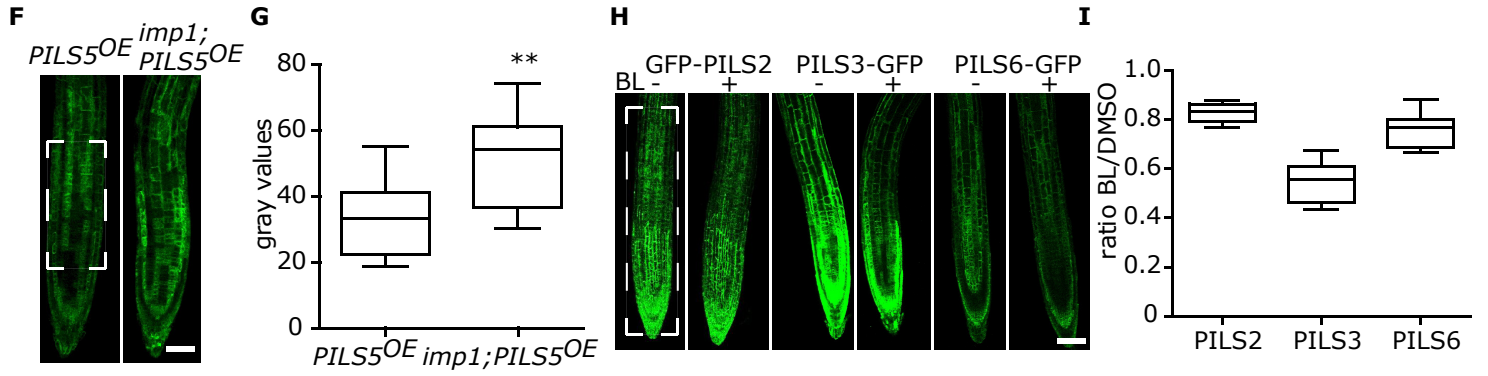
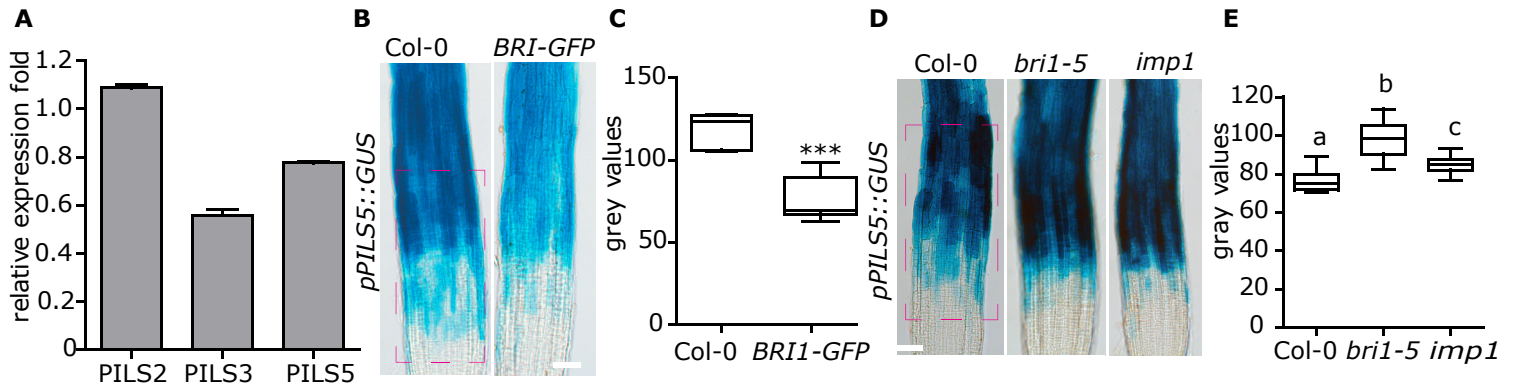


Figure S3. BR signaling negatively impacts on the PILS transcription and protein abundance.
Related to Figure 3.

(A) *PILS* gene expression fold changes in 6-d-old light-grown roots of WT after 2 h of 50 nM BL application. (B-E) GUS images (B, D) and quantifications (C, E) of *pPILS5::GUS* expression pattern in roots of wild type, *BRI1-GFP* overexpressor (B, C), *bri1-5*, and *imp1* (D, E). (n = 8). Scale bars, 140 μ m. (F and G) Confocal images (F) and quantifications (G) of *35S::PILS5-GFP* in 3-d-old roots of WT and *imp1* mutant. (n = 8). Scale bar, 25 μ m. (H and I) Confocal images (H) and quantifications (I) of *35S::GFP-PILS2*, *35S::GFP-PILS3*, and *35S::PILS6-GFP*, which were transferred to plates containing DMSO (solvent control) or 50 nM BL for 5 h. (n = 8). Scale bar, 25 μ m. (J and K) Unprocessed immunoblot using anti-RFP and anti-GFP antibody. See also Figure 3N, 3O. (L-N) Quantifications and relative quantification of 7-d-old root segments of WT, *PILS5^{OE}*, and *bri1* mutants, which were transferred to 21°C (control) and 29°C (HT) for additional 3 days. (n > 25). The dashed boxes represent the ROIs used to quantify the signal intensity. Stars and letters indicate values with statistically significant differences (**P < 0.01, ***P < 0.001, student *t*-test (C and G); P < 0.01, one-way ANOVA (E, L-N)).

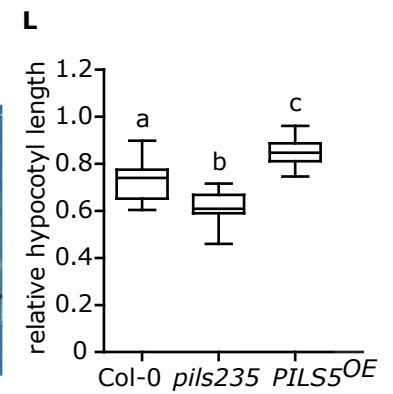
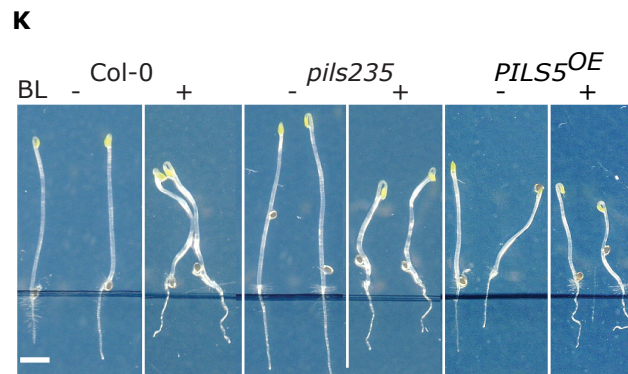
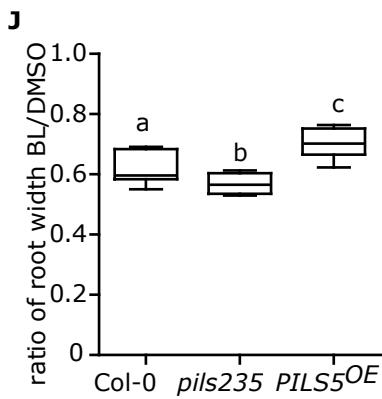
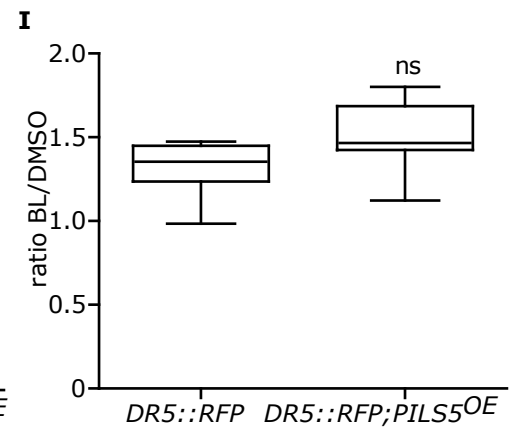
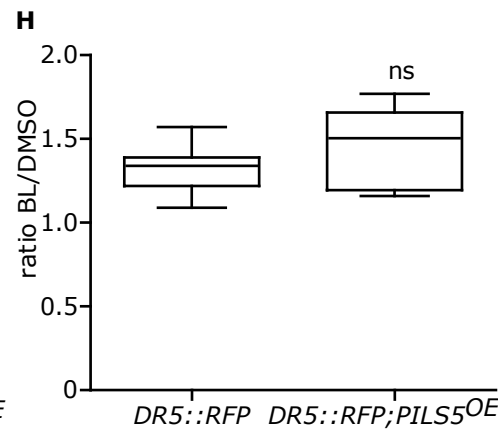
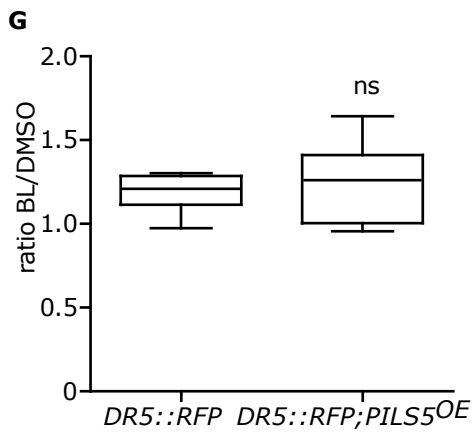
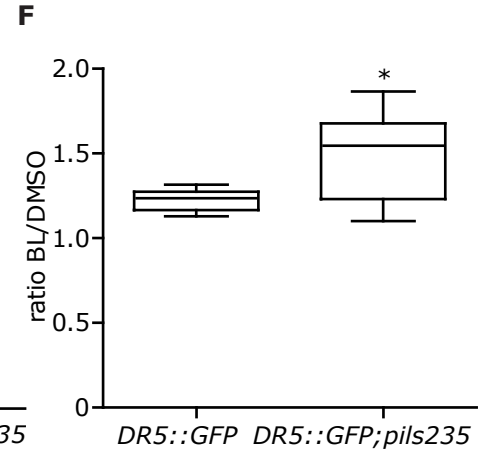
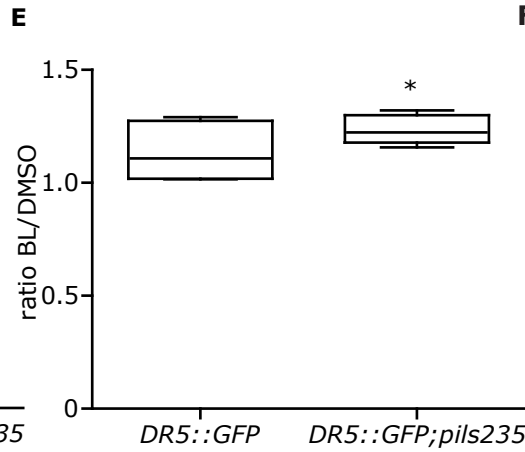
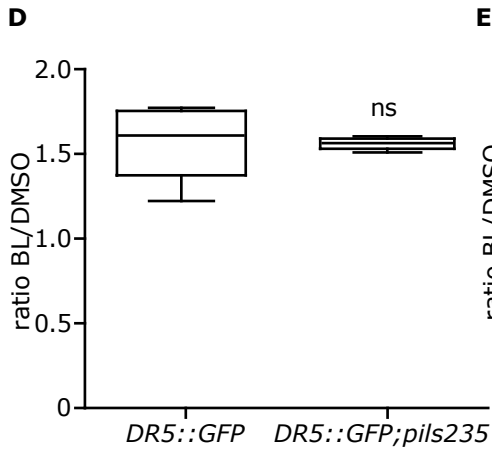
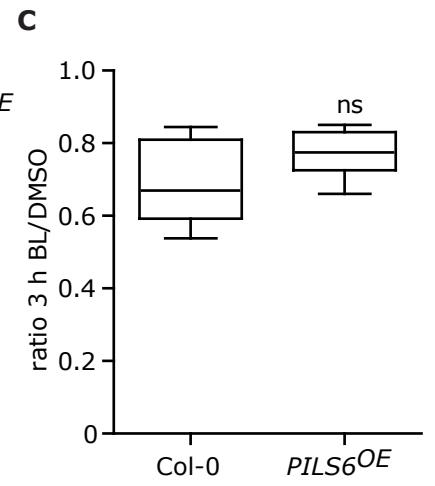
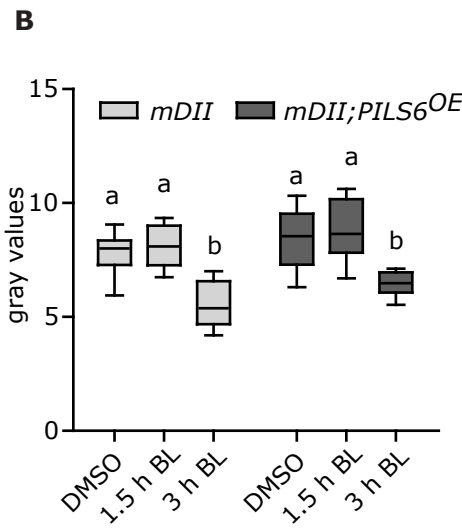
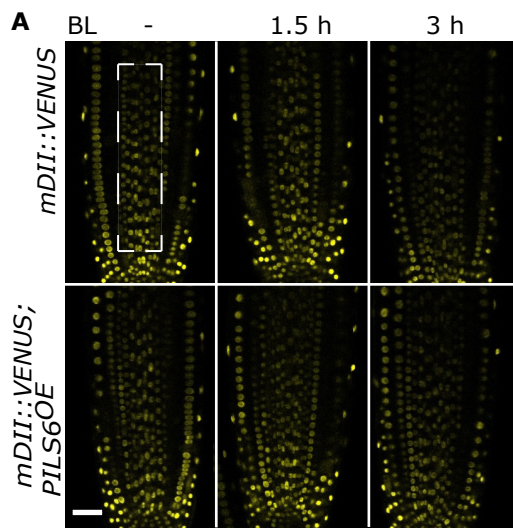


Figure S4. PILS proteins define nuclear auxin responses. Related to Figure 4 and Figure 5.

(A-C) Confocal images (A) and quantifications (B, C) of *mDII-VENUS* in WT and in *PILS6^{OE}* after 1.5 h and 3 h of BL application. (n > 8). Scale bars, 25 μ m. The dashed boxes represent the ROIs used to quantify signal intensity. (D-I) Quantification (ratios) of *DR5::GFP* (D-F) or *DR5::RFP* (G-I) in three replicates, showing a relative increase in auxin response in roots of *pils235* (D-F), but no relative difference in *PILS5^{OE}* (G-I) when treated with 50 nM BL. (n = 8). D and G is the ratios of Figure 4M and 4N, respectively. (J) Quantification of root widths in the meristematic region of 6-d-old light-grown WT, *pils235*, and *PILS5^{OE}* roots. (K and L) Scanned images (K) and quantifications (L) of 5-d-old dark-grown hypocotyls of WT, *pils235*, and *PILS5^{OE}* germinated on plates with DMSO or 100 nM BL. (n > 25). Scale bar, 3 mm. Letters and stars indicate values with statistically significant differences (*P < 0.01, student's *t*-test (C-I), ns: no significant difference; P < 0.01, one-way ANOVA (B, J, and K)).

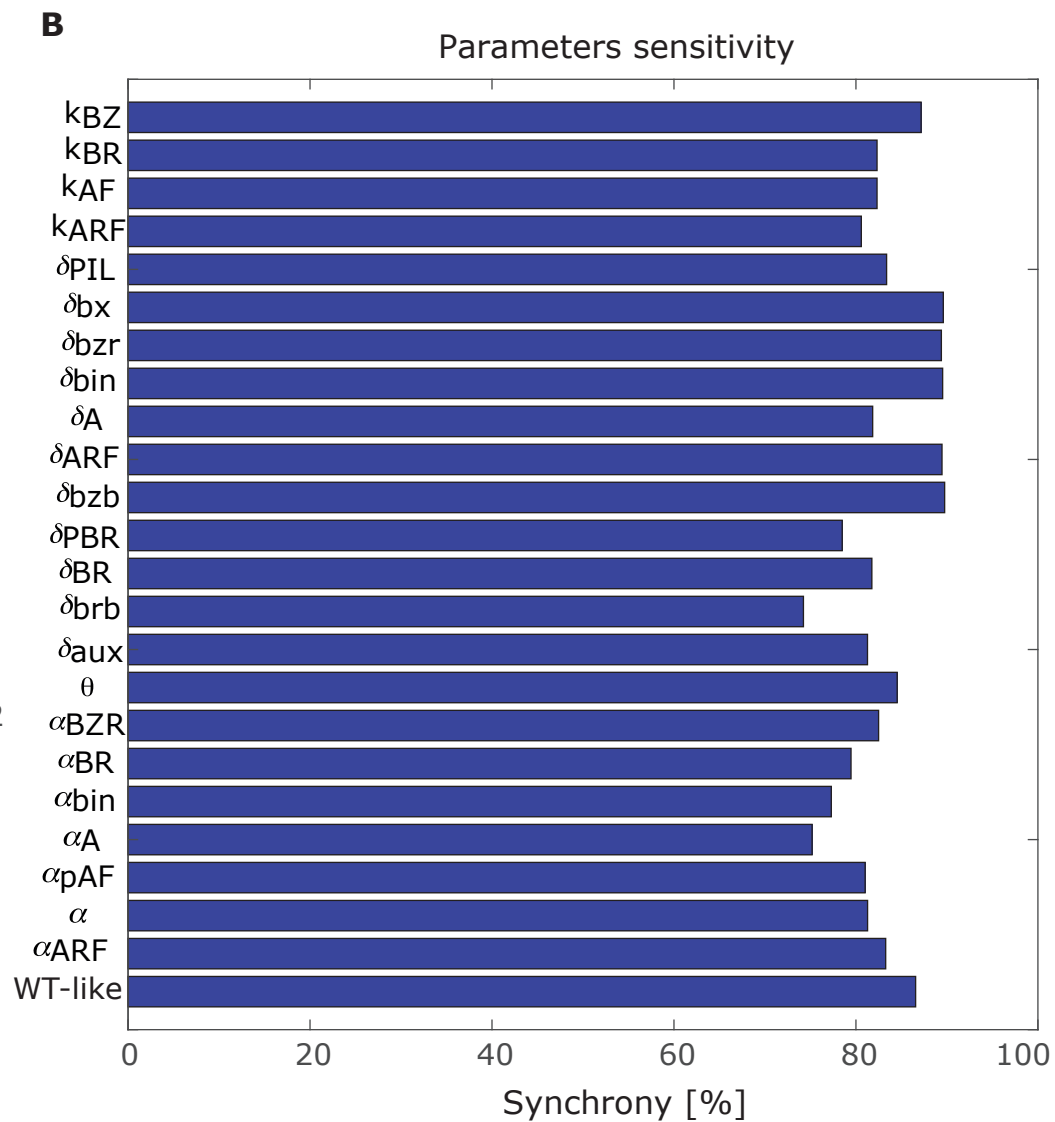
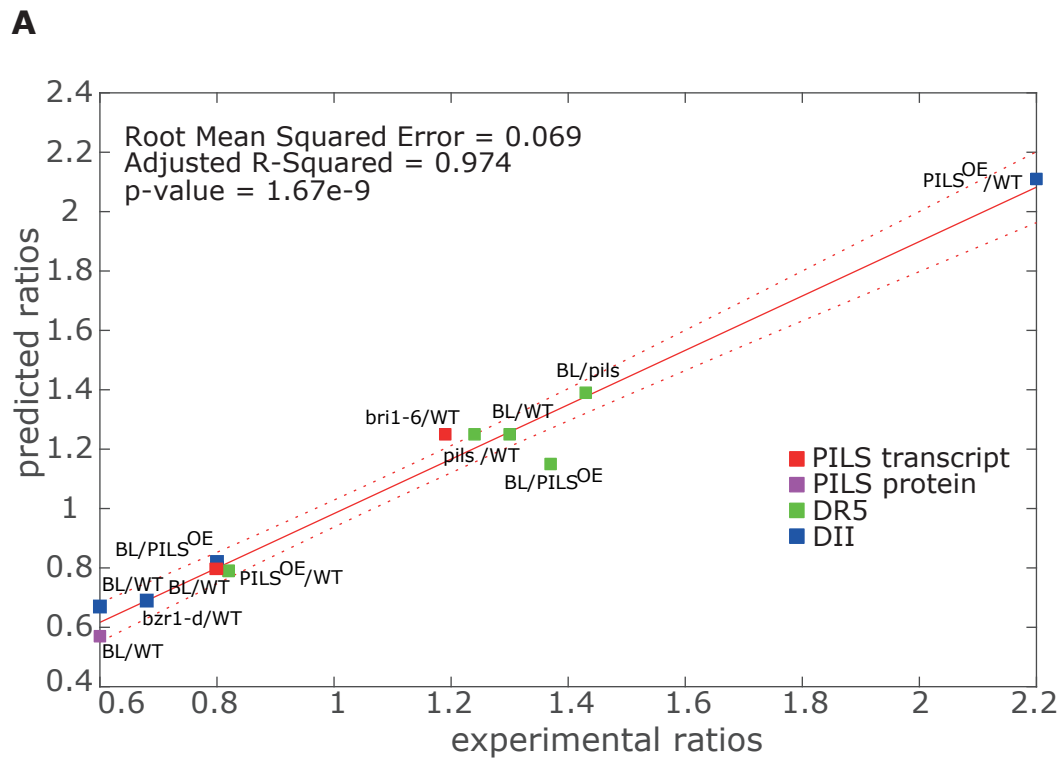


Figure S5. Estimation of model parameters and testing of model robustness to noise. Related to Figure 6.

(A and B) Depict parameter estimation fitness plot. Each predicted ratio was compared to experimental observations to fit a global linear regression model (A) and model robustness based on +/- 25% variation of parameters (B). Synchrony of auxin and BR signaling was plotted against each parameter.

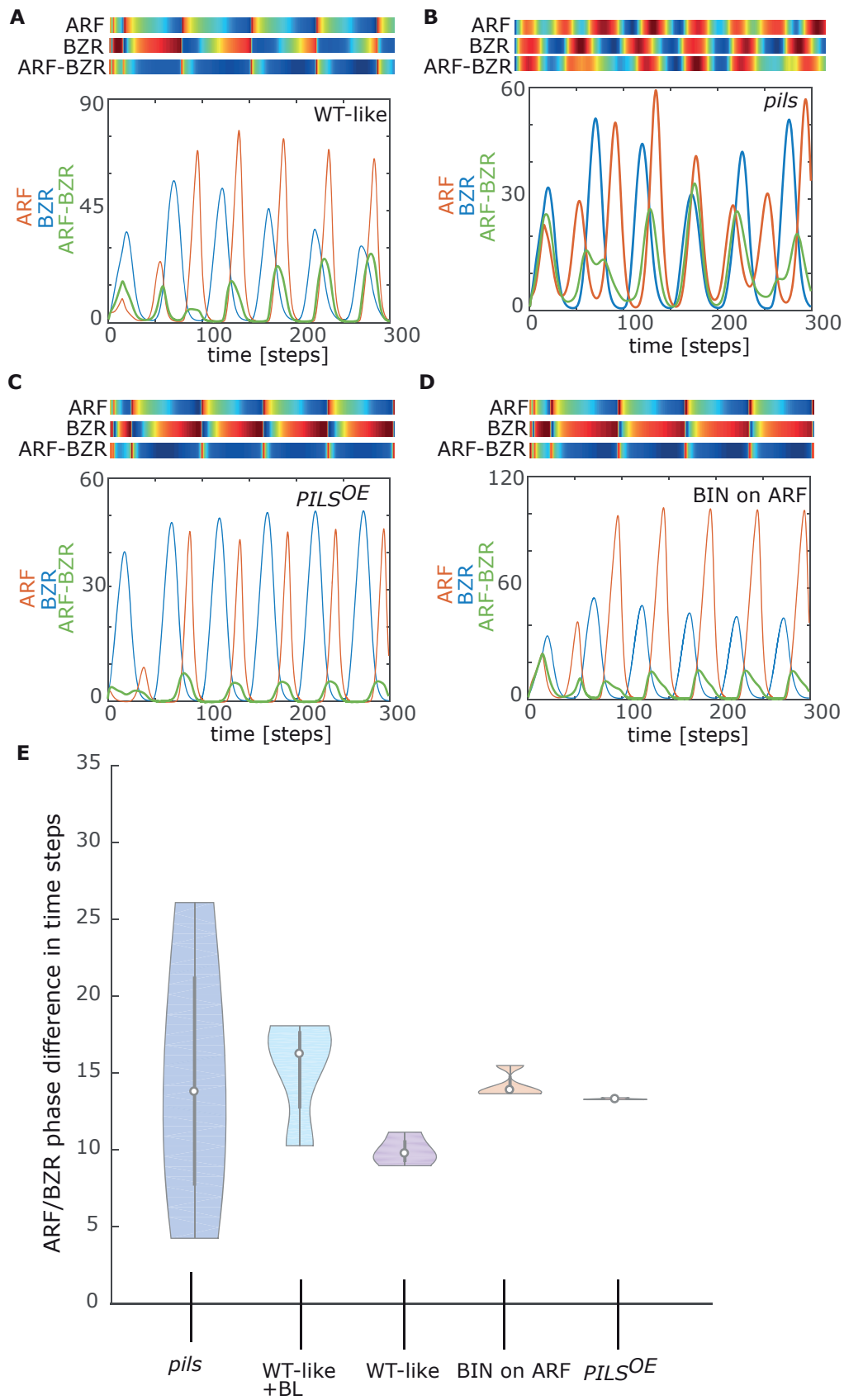


Figure S6. Simulations of computer model predicts the phase locking between BR and auxin signaling outputs through PILS-dependent auxin transport. Related to Figure 6.

(A-D) Model simulations with PILS (A), without PILS-dependent feedback (B) (corresponds to Figure 6A and 6B), as well as with mild (10-fold) *PILS* overexpression (C) and by including BIN2 effect on ARF activation (D). Graphs depict time-lapse for BZR dimers (blue), ARF dimers (red) and ARF-BZR heterodimer (green) levels and corresponding heat maps (blue to red) for peak responses. (E) Violin plots show phase difference between BZR and ARF oscillation, corresponding to model simulations (A-D).

Genotyping primers

pils2-2 FP: ATTGCTCAAGGTGAATCCAT pils2-2 RP: AGACCAATCACGGTTAAACA
Salk_LB1-3: ATTTTGCCGATTTTCGGAAC
pils5-2 FP: CCCTTGTTTGGATCATGGTA pils5-2 RP: TCTTACTGCACCGAAAATGA
pils3-1 FP: AAAGGCATGACGACGGTTAC pils3-1 RP: AAGAGCGTCTCCAAAATTTGG
bri1-301-FP: GGAAACCATTGGGAAGATCA bri1-301-RP: GCTGTTTCACCCATCCAA

Cloning primers

pPILS3-ATTB4_FP: GGGGACAACCTTTGTATAGAAAAGTTGCGGAAGCTAATTCTCTGAGACATAGC
pPILS3-ATTB1_RP: GGGGACTGCTTTTTTGTACAACTTGCCTTTTTACTATCAACGCGAGAATC

qRT-PCR primers

PILS2_qPCR_FP: GTGATGCTTGTACTTGGTGGTATG
PILS2_qPCR_RP: AACTTGAACATTGGATCTGCTGAG
PILS3_qPCR_FP: AGGCGACCATGCAAGTGTTG
PILS3_qPCR_RP: GTGGTACAGCTAGATGACAGTGAG
PILS5_qPCR_FP: TCAGACGGTTACTTGAAGACA
PILS5_qPCR_RP: GAAATGTAAGTCCCATGTTACC
ACTIN2_qPCR_FP: ATTCAGATGCCAGAAAGTCTTGTTT
ACTIN2_qPCR_RP: GCAAGTGCTGTGATTTCTTTGCTCA

ChIP-qPCR primers

IAA19 ChIP-F: GGGAATTTGGTTTACCAGGATG
IAA19 ChIP-R: CTCAAGTATTGGGTTGAATTTTACTTAG
PILS2 ChIP-F: CCGCCGATTCATGCTTTTTAAT
PILS2 ChIP-R: AGACGACAAAAGGGAACGCT
PILS5 ChIP-F: TAATCAGAGGCTACGACGGC
PILS5 ChIP-R: CGAAAACAACTAAATCCCAACTCA
UBC30 ChIP-F: CAAATCCAAAACCCTAGAAACCGAA
UBC30 ChIP-R: AACGACGAAGATCAAGAACTGGGAA

Table S1. Primers used in this study. Related to STAR Methods.